[1]W. A. Harrison, *Pseudopotential in the Theory of Metals* (Benjamin, New York, 1966).
[2]S. H. Vosko, R. Taylor, and G. H. Keech, Can. J. Phys. **43**, 1187 (1965).
[3]R. W. Shaw, Jr., Phys. Rev. **174**, 769 (1968); Ph.D. thesis (Stanford University, 1968) (unpublished).
[4]G. Gilat, G. Rizzi, and G. Cubiotti, Phys. Rev. **185**, 971 (1969).
[5]D. L. Price, K. S. Singwi, and M. P. Tosi, Phys. Rev. B **2**, 2983 (1970).
[6]W. J. L. Buyers and R. A. Cowley, Phys. Rev. **180**, 755 (1969).
[7]H. G. Smith, G. Dolling, R. M. Nicklow, P. R. Vijayaraghawan, and M. K. Wilkinson, in *Neutron Inelastic Scattering* (IAEA, Vienna, 1968), Vol. I, p. 149.
[8]R. Stedman and G. Nilson, Phys. Rev. **145**, 492 (1966).
[9]B. N. Brockhouse, T. Arase, G. Caglioti, M. Sakamoto, R. N. Sinclair, and A. D. B. Woods, in *Inelastic Scattering of Neutrons in Solids and Liquids* (IAEA, Vienna, 1961), p. 531.
[10]R. E. Schmunk, R. M. Brugger, P. D. Randolph, and K. A. Strong, Phys. Rev. **128**, 562 (1962).
[11]R. J. Elliott and H. Stern, Ref. 9, p. 61.
[12]J. J. J. Kokkedee, Physica (Utr.) **28**, 893 (1962); in *Inelastic Scattering of Neutrons in Solids and Liquids* (IAEA, Vienna, 1963), Vol. I, p. 15.
[13]H. Takahashi, Phys. Rev. **172**, 747 (1968).
[14]J. J. J. Kokkedee, Physica (Utr.) **28**, 374 (1962).
[15]A. A. Maradudin and A. E. Fein, Phys. Rev. **128**, 1589 (1962).
[16]G. B. Bjorkman, B. I. Lundquist, and A. Sjolander, Phys. Rev. **159**, 551 (1967).
[17]*Solid State Physics*, edited by F. Seitz, D. Turnbull, and H. Ehrenreich (Academic, New York, 1970), Vol. 24; V. Heine and J. E. Shively, J. Phys. C **4**, 255 (1971).
[18]K. S. Singwi, M. P. Tosi, R. H. Land, and A. Sjolander, Phys. Rev. **176**, 589 (1968); Phys. Rev. B **1**, 1044 (1970).
[19]L. Kleinman, Phys. Rev. **160**, 585 (1967); D. C. Langreth, Phys. Rev. **181**, 753 (1969).
[20]A. W. Overhauser, Phys. Rev. B **3**, 1888 (1971).
[21]F. Toigo and T. O. Woodruff, Phys. Rev. B **2**, 3958 (1970).
[22]D. J. W. Geldart and S. H. Vosko, Can. J. Phys. **44**, 2137 (1966); D. J. W. Geldart and R. Taylor, Can. J. Phys. **48**, 155 (1970); Can. J. Phys. **48**, 167 (1970).
[23]A. J. Pindor and R. Pynn, J. Phys. C **2**, 1037 (1969).
[24]D. Pines and P. Nozières, *The Theory of Quantum Liquids* (Benjamin, New York, 1966).
[25]J. Hubbard, Proc. R. Soc. A **240**, 359 (1957); Proc. R. Soc. A **243**, 336 (1957); L. N. Falicov and V. Heine, Adv. Phys. **10**, 57 (1961).
[26]N. W. Ashcroft, Phys. Lett. **23**, 48 (1966).
[27]E. G. Brovman, Y. U. Kagan, and A. Halos, in *Neutron Inelastic Scattering* (IAEA, Vienna, 1968), p. 164.
[28]D. Weaire, J. Phys. C **1**, 210 (1968).
[29]S. H. Vosko, Phys. Lett. **13**, 97 (1964).
[30]Satya Prakash and S. K. Joshi, Phys. Rev. B **187**, 819 (1969).
[31]A. D. B. Woods and S. H. Chen, Solid State Commun. **2**, 233 (1964).
[32]N. S. Saxena, B. Jhamb, S. C. Jain, and R. C. Bhandari (unpublished).

PHYSICAL REVIEW B VOLUME 7, NUMBER 10 15 MAY 1973

de Haas-van Alphen Effect in Iridium*

S. P. Hörnfeldt,† L. R. Windmiller, and J. B. Ketterson
Argonne National Laboratory, Argonne, Illinois 60439
(Received 2 October 1972)

The de Haas–van Alphen effect has been used to study the extremal areas, cyclotron masses and spin-splitting nulls on the two Γ-centered sheets of the Fermi surface of iridium for the magnetic field in a (110) plane. The measured extremal areas are in good agreement with recent relativistic-augmented-plane-wave calculations by Andersen. The mass-enhancement factor determined from a comparison of the calculated and measured masses was found to be 1.31 and rather isotropic for the Γ6 sheet; the enhancement on the Γ5 sheet is distinctly more anisotropic.

I. INTRODUCTION

The platinum-group transition metals have received a great deal of interest over recent years. Their electronic and magnetic properties have been studied extensively. One characteristic of this group of metals is their high density of states at the Fermi energy, which increases together with the magnetic susceptibility in the sequence Ir, Rh, Pt, and Pd. However, they are unusual in that with the increasing tendency towards ferromagnetism, superconductivity is suppressed. Ir, with a transition temperature of 0.1 °K, is the only one of these metals that has proven to become superconducting.

A detailed knowledge of the electronic band structure in the vicinity of the Fermi level is a necessary foundation for treating electronic, magnetic, and superconducting properties in these metals.

The de Haas–van Alphen (dHvA) effect has been used for experimental investigations of the Fermi surface (FS) and effective cyclotron masses in many metals.[1] Pd[2] and Pt[3] have been exhaustively studied with the dHvA effect; also, the FS of Rh is rather well established experimentally.[4,5] From band-structure calculations[6] the FS of Ir is expected to consist of four different sheets not re-

lated by symmetry. dHvA measurements on the smallest two of these sheets have been published previously.[7-10] Some preliminary results of the present investigation of the two remaining sheets Γ6 and Γ5, of the FS of Ir have been reported recently.[11] Subsequently, Grodski and Dixon[12] reported further dHvA extremal-areas measurements in Ir. In their work the Γ6 surface was observed over a limited range of magnetic field angles while the larger Γ5 surface was only observed for one symmetry direction. In this paper we report complete area measurements and several effective masses in a (110) plane for the Γ6 sheet. We also observed three spin-splitting nulls on this sheet. For the Γ5 sheet we observed dHvA frequencies over about one third of the (110) plane; we have determined three effective cyclotron masses on this sheet.

In Sec. II we review the band-structure calculations for Ir and the resulting FS. In Sec. III we discuss the experimental technique. Our experimental results are presented in Sec. IV and discussed in Sec. V.

II. BAND STRUCTURE AND THE FERMI SURFACE OF Ir

The crystal structure of Ir is face-centered cubic and the Brillouin zone is shown in Fig. 1. The only existing band-structure calculation for Ir can be found in the work by Andersen,[6] in which he carried out relativistic-augmented-plane wave (RAPW) calculations for the Pt-group transition metals. For Ir a $5d^7\,6s^2$ potential together with full Slater exchange was used. (see *Note added in proof.*) The energy levels at symmetry points were calculated and the energy bands were sketched using the Pt calculations as a guide; the resulting bands are shown in Fig. 2. In addition, the k vectors on three constant-energy surfaces associated with three values of the energy in the immediate vicinity of the Fermi energy were calculated in detail. At each energy the number of carriers and the electronic density of states, as well as the areas and effective masses of the various dHvA orbits, were then obtained by numerical integrations. The Fermi energy was determined by interpolating the energy to a value such that the difference between the volumes of the hole and electron sheets corresponded to one state per atom. The band structure, Fig. 2, predicts four sheets to the Fermi surface and we will now discuss these sheets in the order of increasing number of carriers. The $X3$ band lies above the Fermi energy but drops below E_F as we move away from this point in any direction. Thus, this band gives rise to a hole sheet centered at X that is closed and, since it lies near a band extremum, it should be nearly ellipsoidal in shape. The $X4$ band also drops below E_F when moving away from X, resulting in a second closed-hole pocket centered at X. This larger $X4$ pocket is, however, much more nonellipsoidal in shape than the smaller $X3$ pocket. The sheet containing the next largest number of carriers is the electron surface associated with the Γ6 level. This sheet is closed and centered at Γ and its extension in the [100], [110], and [111] directions are given by the intersections of the levels Δ6, Σ6, and Γ6 with the Fermi level. Figure 3 shows this sheet along with the central extremal orbits for fields parallel to [100], [110], and [111]. (This sheet was actually drawn for the case of Pt. The Ir sheet is, however, nearly identical in shape although it is about 15% smaller.) The sheet with the largest number of carriers is associated with the Γ5 level and this sheet is also a closed electron sheet centered at Γ. As can be seen in Fig. 2, its extension along ΓK almost intersects the zone boundary and is longer than the extensions along ΓX and ΓL. Thus, this sheet

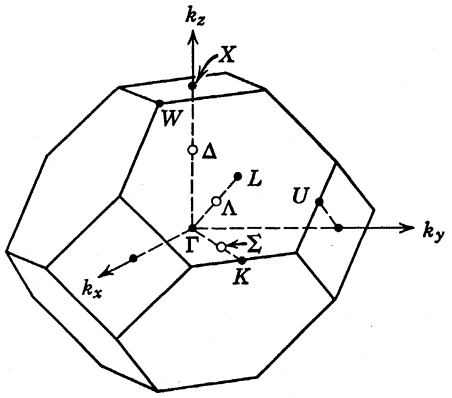

FIG. 1. Brillouin zone for fcc lattice with standard notations for symmetry points.

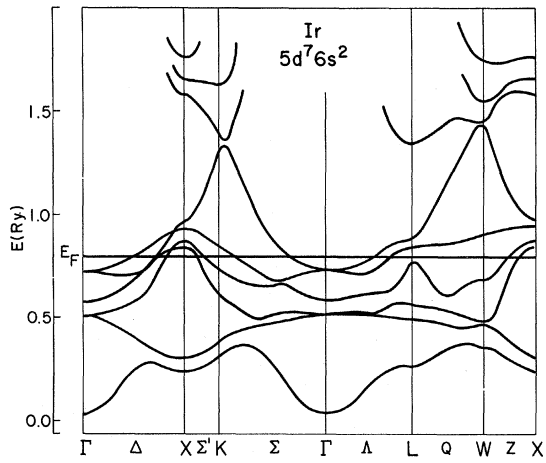

FIG. 2. Outline of the energy bands of Ir as determined by Andersen (Ref. 22).

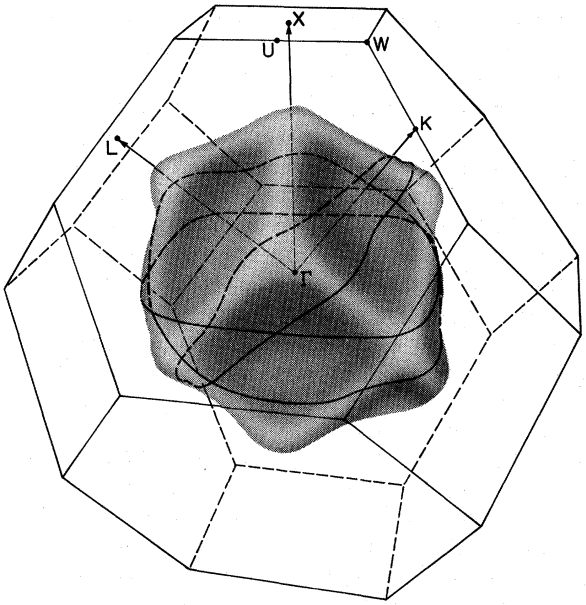

FIG. 3. The Γ6 sheet of the Fermi surface of Pt. The anisotropy of the Γ6 sheet in Ir is very similar with the Fermi radii about 15% smaller. Shown are the extremal areas for the magnetic field parallel to ⟨100⟩, ⟨110⟩, and ⟨111⟩.

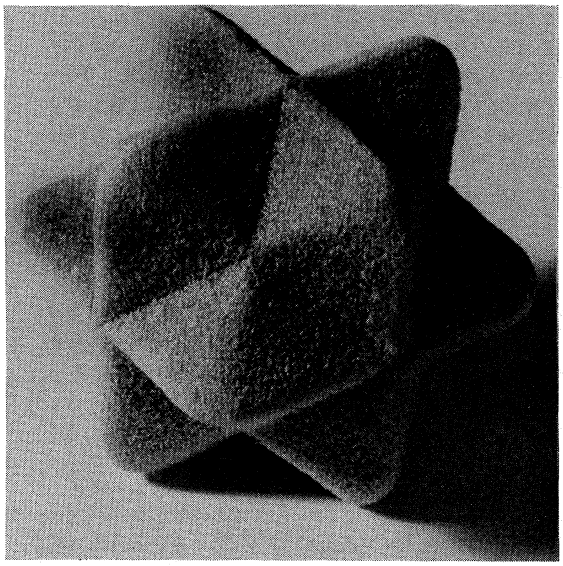

FIG. 4. Model of the Γ5 sheet in Ir.

is rather anisotropic with pronounced "bumps" in the [110] directions. Figure 4 shows a photograph of a model of this sheet. Cross sections of the four predicted sheets of the FS of Ir are shown in Fig. 5.

Both the Γ5 and Γ6 sheets have more than one extremal cross section for some field directions. As the sheets have inversion symmetry, the central section (which includes the point Γ) is always extremal. For field directions where the central area is a minimum as a function of k_H (the momentum along $\hat{H}$) there must be a maximum area for some value of k_H and thus a second extremal area since these sheets are closed. (In general there must be an even number of extremal areas in this case.) For the Γ6 sheet near [111] and for the Γ5 sheet near [110] and near 25° from [100] in a (110) plane we have examples of the case

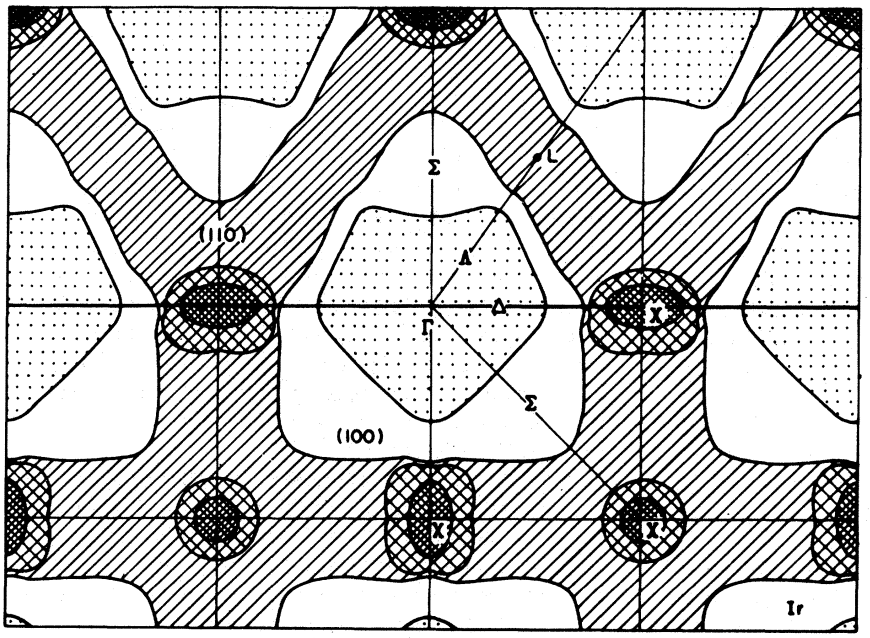

FIG. 5. Cross sections of the predicted Fermi surface sheets of Ir in the central (100) and (110) planes (Ref. 6).

where there are two extremal cross sections. The two frequency branches associated with these two extremal areas must merge at some angle. The smaller of the two frequencies is, of course, the central section. For the case where the central section is maximal with respect to k_H the total number of extremal cross sections must be odd (including one) for a closed sheet. For the field along [100] the $\Gamma 5$ sheet supports three extremal orbits. The angular dependence of these three extremal areas is illustrated in Fig. 9. The two noncentral extremal areas merge and then cease to exist when the magnetic field is tipped away from [100].

III. EXPERIMENTAL TECHNIQUE

The measurements to be reported here were carried out using the large-amplitude low-frequency field-modulation technique.[13,14] The experimental apparatus has been discussed elsewhere.[15] Briefly, it consists of a 72-kG superconducting solenoid together with a system capable of either ^{3}He or ^{4}He evaporative cooling. The magnetic field was calibrated with NMR and was found to be proportional to the magnet current and reproducible to within 0.02% between 25 and 50 kG.

The absolute dHvA frequencies were measured by varying the magnitude of the magnetic field while keeping its direction constant (field sweep). The angular dependence was most accurately determined by rotating the sample at a constant magnetic field (field rotation). The detected dHvA signal was recorded on a strip-chart recorder.

The field sweeps were carried out in the following way. The magnet current was swept at a very low rate corresponding to one dHvA oscillation per minute or slower; a magnet current reading was taken and a counter (counting the number of dHvA oscillations) was set as the pen of the recorder passed its zero line. The sweep rate was then increased ten to one-hundred times depending on the signal-to-noise ratio of the dHvA signal and 300–1500 oscillations recorded. At the end of the field sweep, the sweep rate was decreased and another reading of the magnet current taken (together with the number of oscillations) as the recorder pen passed its zero line. We found that the dHvA frequencies determined in this way were reproducible to within 0.2%.

During the field-rotation measurements the sample was rotated at a rate of 0.2°–1°/min and every degree of rotation was marked on the recorder trace. The relative accuracy of the angular determinations was about 0.2°.

The effective cyclotron masses were determined from the temperature dependence of the amplitude of the dHvA oscillations. For these measurements precise temperature determinations are required. For the ^{4}He temperature range the sample was immersed in a static column of ^{4}He which was in thermal contact with a second ^{4}He bath which was pumped to the desired temperature. The pressure of the sample bath was then accurately monitored using a Texas Instruments precision pressure gauge. For the case of measurements at ^{3}He temperatures, the sample was surrounded by ^{3}He which was pumped to the desired temperature. The pressure drop across the pumping line can then lead to errors. To circumvent this problem a carbon resistance thermometer, which was calibrated as a function of field, was used to determine the sample temperature.

The samples were right-circular cylinders 1 mm in diameter and about 5 mm in length and were grown from Johnson Matthey[16] 99.999%-pure Ir using an electron-beam floating-zone refiner. The residual resistivity ratio of the samples was over 2000. Details of the growing and annealing procedures can be found elsewhere.[17,9]

IV. EXPERIMENTAL RESULTS

A. General

The dHvA frequencies were studied for the magnetic field in a (110) plane. The sample was carefully oriented so the magnetic field was always within 0.5° of the (110) plane. The orientations were checked by recording the dHvA frequencies from the $X3$ pockets. Two of these pockets are degenerate in the (110) plane so the beat between these two frequencies gave a precise measurement of the deviation of the magnetic field from the (110) plane. As both the $\Gamma 5$ and $\Gamma 6$ sheets have the full symmetry of the cubic point group, their dHvA frequencies are stationary with respect to magnetic field deviation from a (110) plane. A deviation of less than 0.5° introduces a negligible error and our results on the $\Gamma 5$ and $\Gamma 6$ sheets are valid for the (110) plane within our other experimental errors. dHvA signals from all four predicted sheets of the FS were observed. With the magnetic field in the [100] direction all eight of the expected dHvA frequencies were detected. Five of these frequencies could be made to be dominant in the dHvA signal by detecting on different harmonics of the modulation frequency and adjusting the modulation amplitude as discussed in Ref. 14. The three remaining frequencies were determined from beat patterns.

Since rather extensive experimental studies of the two sets of X-centered pockets have been previously published,[7–10] we limited our investigation of these sheets mainly to extremal areas in symmetry directions. The results obtained, summarized and compared with theoretical values[18] in

Table I, agree very well with other experimental results, especially those recently reported by Grodski and Dixon.[12] The existence of a noncentral extremal area on the $X4$ pocket in the vicinity of [110] reported by Grodski and Dixon[12] was confirmed. Figure 6 shows our area results for this pocket in the region between [111] and [110], in the (110) plane. We determined the cyclotron effective masses for the central and noncentral orbits of the principal $X4$ pockets at [110]. Both these masses (Table I) gave an enhancement factor of 1.3.

B. Γ6 Sheet

For the Γ6 sheet, dHvA areas were observed for all magnetic field directions in the plane investigated except where spin-splitting nulls occurred. Figure 7 shows the angular dependence of the Γ6 extremal areas. For the magnetic field in the vicinity of [111] the sheet supports two extremal cross sections, the smaller of these being the central cross section. As the noncentral area gave the dominant dHvA frequency, the central area (indicated with pluses) was determined from the beat frequency in field-sweep measurements. Figure 8 shows the measured effective masses of this sheet. All these masses were measured in the temperature range 1.05–1.5 K using ^{4}He. Three spin-splitting nulls were observed for this sheet and are indicated by the arrows in Figs. 7 and 8. Table I gives the extremal areas and masses for the magnetic field along symmetry directions compared with theoretical calculations.[18]

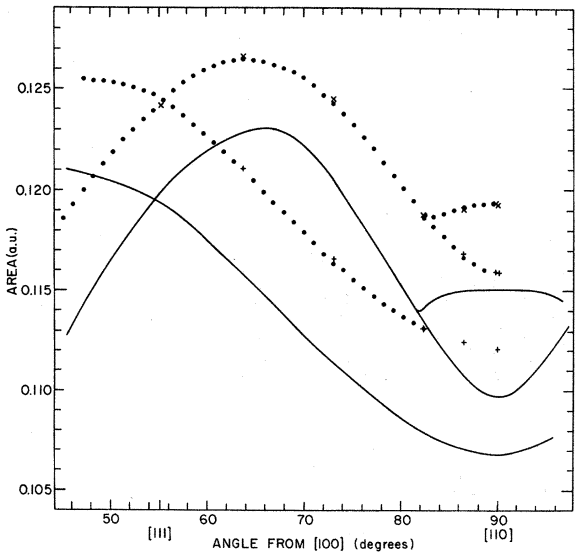

FIG. 6. Angular dependence of the extremal areas of the $X4$ pockets in the region ⟨111⟩ to ⟨110⟩ in the (110) plane. The solid line shows the variation predicted by theory. The filled circles (●) refer to field-rotation measurements, the crosses (×) to field sweeps, and the pluses (+) are derived from beats in field sweeps.

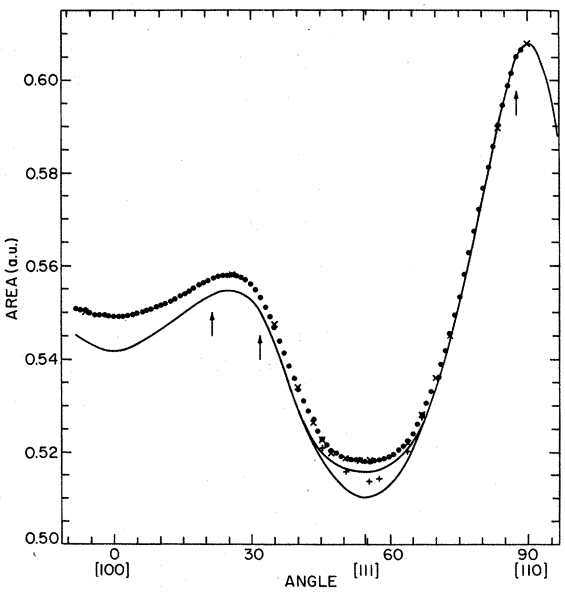

FIG. 7. Angular dependence of the extremal area for the Γ6 electron sheet observed in the (110) plane. The solid line shows the variation predicted by theory. The filled circles (●) are obtained in field-rotation measurements, the crosses (×) from field sweeps, and the pluses (+) from beats in field-sweep measurements. The arrows indicate orientations where spin-splitting nulls were observed.

C. Γ5 Sheet

For the Γ5 sheet dHvA oscillations were detected only for the magnetic field in directions where the angular dependence of the extremal areas was small. Figure 9 shows our extremal-area results for this sheet. The general features of the angular dependence of the central extremal area of this sheet in the (110) plane are the following: (i) a maximum with the magnetic field along [100]; (ii) a minimum about 25° away from [100]; (iii) a maximum again at [111]; and (iv) a minimum at [110]. For the field directions where the angular dependence is the largest it is necessary to be able to resolve up to 150 dHvA oscillations per degree. That means that the crystal has to be perfect (i.e., no bending or mosaic spread) within about ± 0.002°; the magnetic field direction must be uniform over the sample within the same limit. These conditions were not always fulfilled. The anisotropy of the sheet is such that two extremal areas exist around the two minima in the angular dependence. Around [100] we observed the large central area and also the two noncentral areas discussed in Sec. II. The smaller of these noncentral areas gave a signal strong enough to allow

TABLE I. Comparison of experimental results with RAPW band calculations by Andersen and Mackintosh (Ref. 18).

		Extremal areas (a.u.)				Cyclotron effective masses (m^*/m_0)				Mass-enhancement factor
		Central orbits		Noncentral orbits		Central Orbits		Noncentral orbits		
		Theory	Expt.	Theory	Expt.	Theory	Expt.	Theory	Expt.	
–	[100]	0.541	0.5492 ± 0.0005			1.75[a]	2.25 ± 0.02			1.29
Γ6	[110]	0.607	0.6062 ± 0.0010			1.86	2.46 ± 0.01			1.30
	[111]	0.510	0.5138 ± 0.0005	0.516	0.5180 ± 0.0005	1.34		1.47	1.88 ± 0.02	1.28
	[100]	1.507	1.425 ± 0.005	0.872	0.873 ± 0.001	2.55		1.86	2.47 ± 0.01	1.33
				0.880	0.877 ± 0.001			2.04	...	
Γ5	[110]	1.162	1.170 ± 0.002	1.190	1.193 ± 0.002	2.26		2.49	2.99 ± 0.04	1.20
	[111]	1.448	...			3.02				
	[100]	0.0261	0.01832 ± 0.0004			0.21	0.228 ± 0.003[b]			1.1
		0.0388	0.02884 ± 0.0005			0.24	0.28 ± 0.01[b]			1.2
$X3$	[110]	0.0293	0.02135 ± 0.0005			0.22	0.26 ± 0.01[b]			1.2
		0.0405	0.02973 ± 0.0006			0.26	0.31 ± 0.01[b]			1.2
	[111]	0.0318	0.02294 ± 0.0004			0.22	0.25 ± 0.01[b]			1.1
	[100]	0.0915	0.1013 ± 0.0002			0.65	0.91 ± 0.02[b]			1.4
		0.1467	0.1483 ± 0.0005			1.05				
$X4$	[110]	0.1065	0.1121 ± 0.0003			0.76				
		0.1098	0.1159 ± 0.0002	0.1150	0.1193 ± 0.0002	0.72	0.93 ± 0.01	0.78	0.98 ± 0.01	1.3
	[111]	0.1195[a]	0.1242 ± 0.0002			0.83	1.28 ± 0.06[b]			1.5

[a]Recomputed values.

[b]Taken from Ref. 9.

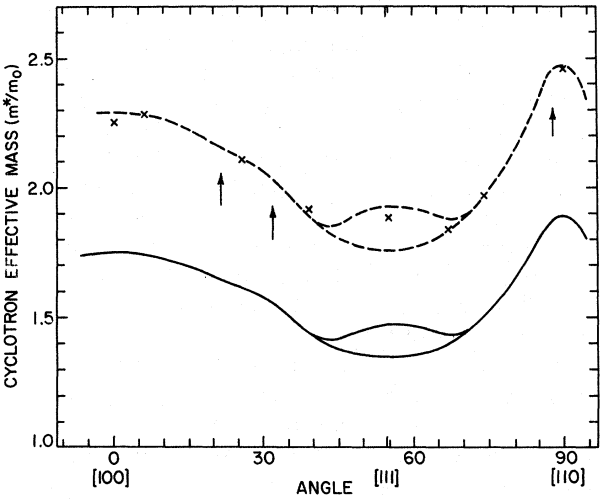

FIG. 8. The angular dependence of the cyclotron effective mass for the Γ6 electron sheet observed in the (110) plane. The solid line shows the variation predicted by theory. The dashed line was obtained by multiplying the theoretical values by a factor of 1.31. The crosses (×) give the experimental results. The arrows indicate orientations where spin-splitting nulls were observed.

field-rotation measurements to be carried out over an interval of 7°. The effective cyclotron mass of this orbit was determined to be $2.51m_0$ using ^{4}He. Near the minimum 25° away from [100] we detected rather strong signals from both the central and noncentral cross sections. The cyclotron effective mass was determined at the minimum of the angular dependence of the noncentral orbit to be $3.34m_0$ using ^{3}He. At [111] we were not able to detect any dHvA oscillations from this sheet. The most likely reason was that the Γ6 sheet gave very strong signals in this region and the third harmonic of the Γ6 frequencies was close to the expected frequency of the Γ5 sheet. Around [110] field-rotation measurements were carried out on the dominant signal from the noncentral extremal area, and the area of the central cross section was determined from beats occurring in long field sweeps. The effective cyclotron mass of the noncentral extremal orbit was determined to be $3.00m_0$ using ^{3}He. A summary and comparison with theory[18] of areas and masses determined with the magnetic field in symmetry directions is given in Table I.

V. DISCUSSION

To achieve a detailed comparison between our experimental results and the band-structure calculation for iridium,[6,18] we used the calculated radii for three different energies in the vicinity of E_F at 35 and 43 directions in the basic $\frac{1}{48}$th of the unit sphere for the Γ6 and Γ5 sheets, re-

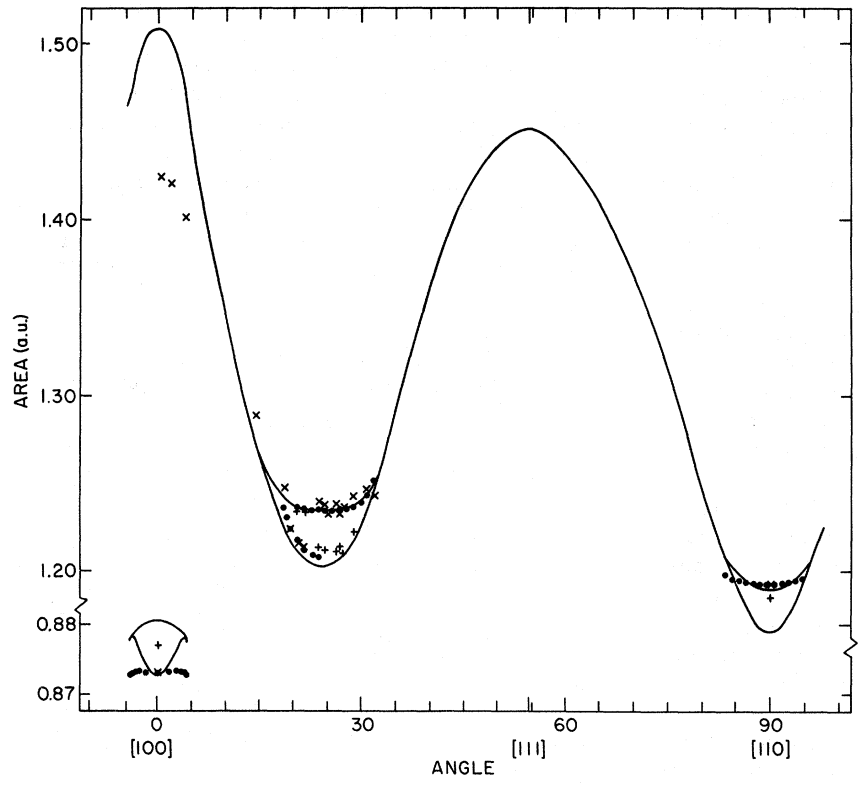

FIG. 9. The angular dependence of the extremal area for the Γ5 electron sheet observed in the (110) plane. The solid line shows the variation predicted by theory. The filled circles (●) are obtained from field-rotation measurements, the crosses (×) from field-sweep measurements, and the pluses (+) from beats in field-sweep measurements.

spectively.[19] Quadratic interpolation gave us the radius and its derivative with respect to energy at these directions for $E = E_F$. A computer program was set up to compute, for a given magnetic field direction, the area and the effective mass of an orbit whose plane was at any chosen distance from the inversion center; interpolation was used to find the appropriate radius and its derivative at every point integrated.

The program was used to trace out the central areas and their effective masses at two degree intervals in a (110) plane using 180 points per area or mass. The noncentral extremal areas and their effective masses were obtained by computing the area and effective mass as function of k_H for those field directions where noncentral extremal areas had been observed.

The solid line in Fig. 7 gives the computed extremal areas for the $\Gamma 6$ sheet in the (110) plane. Our results indicate that the $\Gamma 6$ sheet is somewhat more isotropic than expected from the calculations. The deviation of the theoretical curve from the experimental points varies between zero and about 1%, the experimental areas being consistently the larger. Assuming that the experimental areas are on the average 0.5% larger than the theoretical (in agreement with the results of Grodski and Dixon[12]), we get the volume of this sheet to be 0.75% larger than the volume of the calculated sheet. That is, the $\Gamma 6$ sheet contributes 0.242 states/atom to the carrier concentration.

The solid line in Fig. 8 gives the computed effective cyclotron masses for the $\Gamma 6$ sheet. The average ratio between the experimental masses and the theoretical values is 1.31. The dashed line in Fig. 8 is obtained by multiplying the theoretical masses by this number. This line indicated that the enhancement factor for the $\Gamma 6$ sheet is quite isotropic and lower than the enhancement factor 1.37 determined by specific-heat measurements.[20,21]

As the topology of the $\Gamma 6$ sheet seems to agree so well with that predicted, and the enhancement factor is isotropic, we can obtain an estimate of the $\Gamma 6$ contribution to the density of states by multiplying the calculated density of states[6] (3.3 states/atom Ry) by the enhancement factor. This gives us 4.3 states/atom Ry.

We observed two spin-splitting nulls clearly at 21.7° and 32.0° from [100] in the field-rotation measurements. In the region from 2° to 7° away from the [110] axis the signal was rather weak, so the location of possible spin-splitting nulls in this region was not obvious. However, we could with some certainty locate one spin-splitting null at 2.0° from the [110] axis. It might be that the weakness of the signal in this region was partly due to several rather closely spaced spin-splitting nulls, similar to the situation observed in Pt (see Fig. 13 of Ref. 3). Our observations of spin-splitting nulls on the $\Gamma 6$ sheet suggests that the anisotropy of the g factor of Ir could be similar to that in Pt. Using the dashed curve in Fig. 8 to determine the effective masses for the three field directions where the spin-splitting nulls occurred, we obtain the values 2.3, 2.5, and 2.0 for the g factor. The last value is in fair agreement with the value 2.1 given by Grodski and Dixon[12] for a nearby orientation using an estimated effective mass of $2.4 m_0$.

The solid line in Fig. 9 shows the computed extremal areas for the $\Gamma 5$ sheet in the (110) plane. There is a close agreement between theoretical and measured areas except for the large [100] area where the measured area is 5% smaller. If we take the result of Grodski and Dixon[12] that the two sets of hole pockets contains 0.004 states/atom more than predicted and our estimate that the $\Gamma 6$ sheet contains 0.002 electrons/atom more than predicted, we find that the $\Gamma 5$ sheet also must contribute 0.002 electrons/atom more than the theoretical value of 0.8370 electrons/atom. For this large sheet this correction is a very small relative adjustment to its volume. The above leads us to conclude that the $\Gamma 5$ sheet is more spherical and has less pronounced bumps in the [110] directions than the calculated sheet; it has, however, nearly the same volume.

The two noncentral orbits observed for field directions near [100] exist because the surface of the $\Gamma 5$ sheet is distorted due to the proximity of van Hove singularities in the band structure. Andersen has discussed this situation in detail for the corresponding Fermi-surface sheets in Rh and Pd.[6,22] The measured area of the smaller of these noncentral orbits agrees extremely well with the calculated value but its angular dependence is less drastic; also the difference between the areas of the two non-central orbits is just half of

TABLE II. Cyclotron effective masses for the $\Gamma 6$ and $\Gamma 5$ electron sheets in Ir in the (110) plane.

	Angle from ⟨100⟩ in degrees	Cyclotron effective masses m^*/m_0 Theory	Expt.	Enhancement factor
$\Gamma 6$	0.0	1.75	2.25 ± 0.02	1.29
	6.2	1.74	2.29 ± 0.02	1.32
	25.8	1.61	2.11 ± 0.01	1.31
	39.3	1.44	1.94 ± 0.01	1.35
	55.6[a]	1.47	1.88 ± 0.02	1.28
	67.1	1.40	1.83 ± 0.02	1.31
	74.4	1.50	1.97 ± 0.01	1.31
	90.0	1.89	2.46 ± 0.01	1.30
$\Gamma 5$	0.0[a]	1.86	2.47 ± 0.01	1.33
	24.8[a]	2.54	3.35 ± 0.04	1.32
	90.0[a]	2.49	2.99 ± 0.04	1.20

[a]Noncentral orbits.

the calculated difference. These facts also lead us to the conclusion that the anisotropy of the surface is smaller than predicted.

The mass-enhancement factor for the three masses measured on the $\Gamma 5$ surface (Table II) varies from 1.20 to 1.33. As the other sheets also have enhancement factors of this order or less, we have to assume that the missing parts of the $\Gamma 5$ sheet must have a higher enhancement to account for the value 1.37 obtained by electronic specific-heat experiments.[20,21]

Note added in proof. More recent band calculations for Ir [J. Phys. F 2, 1033 (1972)] show that the Fermi-surface dimensions are very sensitive to the choice of the exchange parameter α, particularly where the d character of the bands is pronounced. These calculations also demonstrate that full Slater exchange give far better agreement with experimental results than a lower value of α; e.g., $\alpha = \frac{2}{3}$.

ACKNOWLEDGMENT

We would like to thank Professor O. K. Andersen for providing us with the RAPW radius vectors of the Ir Fermi surface.

*Work performed under the auspices of the U. S. Atomic Energy Commission.

†Visiting scientist from University of Uppsala, Uppsala, Sweden.

[1]A. P. Cracknell, Advan. Phys. 18, 681 (1969); 20, 1 (1971).

[2]L. R. Windmiller, J. B. Ketterson, and S. Hörnfeldt, Phys. Rev. B 3, 4213 (1971).

[3]J. B. Ketterson and L. R. Windmiller, Phys. Rev. B 2, 4813 (1970).

[4]P. T. Coleridge, Proc. Roy. Soc. (London) A295, 476 (1966).

[5]J. B. Ketterson, L. R. Windmiller, and S. Hörnfeldt, Phys. Letters 26A, 115 (1968).

[6]O. K. Andersen, Phys. Rev. B 2, 883 (1970).

[7]J. J. Grodski and A. E. Dixon, Solid State Commun. 7, 735 (1969).

[8]S. Hörnfeldt, Solid State Commun. 8, 673 (1970).

[9]S. Hörnfeldt, A. Hammerström, K. Carrander, and G. Björck, J. Phys. Chem. Solids 32, 753 (1971).

[10]N. V. Volkenshtein, V. A. Novoselov, V. E. Startsev, and Yu. N. Tsiovkin, Zh. Eksperim. i Teor Fiz. 60, 1773 (1971) [Soviet Phys. JETP 33, 959 (1971)].

[11]S. P. Hörnfeldt, L. R. Windmiller, and J. B. Ketterson, Bull. Am. Phys. Soc. 17, 280 (1972).

[12]J. J. Grodski and A. E. Dixon, Phys. Rev. B 6, 1198 (1972).

[13]A. Goldstein, S. J. Williamson, and S. Foner, Rev. Sci. Instr. 36, 1356 (1965).

[14]R. W. Stark and L. R. Windmiller, Cryogenics 8, 272 (1968).

[15]L. R. Windmiller and J. B. Ketterson, Rev. Sci. Instr. 39, 1672 (1968).

[16]Johnson Matthey Chemicals Limited, 74 Hatton Garden, London, E.C. 1, England.

[17]S. Hörnfeldt, J. B. Ketterson, and L. R. Windmiller, J. Cryst. Growth 5, 289 (1969).

[18]O. K. Andersen and A. R. Mackintosh, Solid State Commun. 6, 285 (1968).

[19]We are indebted to Dr. O. K. Andersen for communicating these unpublished results of his calculations.

[20]K. Clusius and C. G. Losa, Z. Maturf. 10, 545 (1955).

[21]W. L. McMillan, Phys. Rev. 167, 331 (1968).

[22]O. K. Andersen, thesis (Technical University of Denmark, 1969) (unpublished).

PHYSICAL REVIEW B VOLUME 7, NUMBER 10 15 MAY 1973

Exchange and Correlation in the Electron Gas

L. J. Sham

IBM Thomas J. Watson Research Center, Yorktown Heights, New York 10598

*Department of Physics, University of California, San Diego, La Jolla, California 92037**

(Received 22 December 1972)

Recent theories of Singwi *et al.* for the dielectric response beyond the random-phase approximation are examined in the density-functional formalism. Their approximation and another from the perturbation expansion in the electron-electron interaction are used to calculate the correction to the local-density approximation of the exchange energy in atoms. The latter gives better results.

I. INTRODUCTION

Singwi and co-workers have, in a series of papers,[1–3] given approximations for the dielectric function of the electron gas beyond the random-phase approximation. Their results for the pair distribution are rather superior in that they only become slightly negative at small distances for $r_s \gtrsim 5$. The latest version by Vashishta and Singwi[3] also satisfies the compressibility sum rule in the sense that the value of the compressibility coming from the long-wavelength limit of the dielectric function agrees with the second derivative of the total energy. The most striking success of the

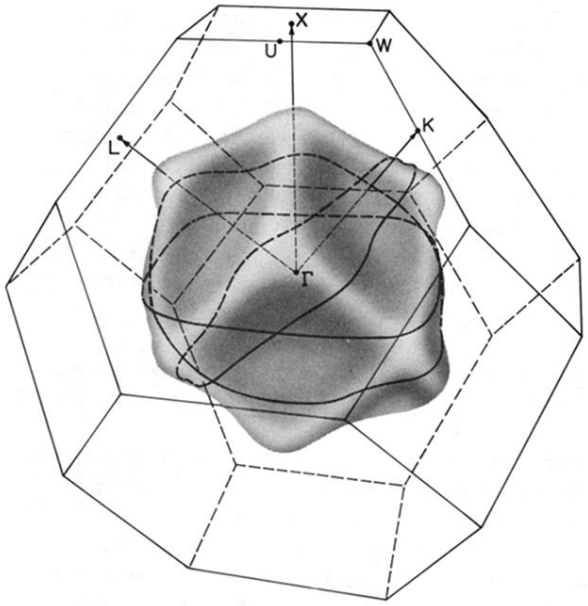

FIG. 3. The Γ6 sheet of the Fermi surface of Pt. The anisotropy of the Γ6 sheet in Ir is very similar with the Fermi radii about 15% smaller. Shown are the extremal areas for the magnetic field parallel to ⟨100⟩, ⟨110⟩, and ⟨111⟩.

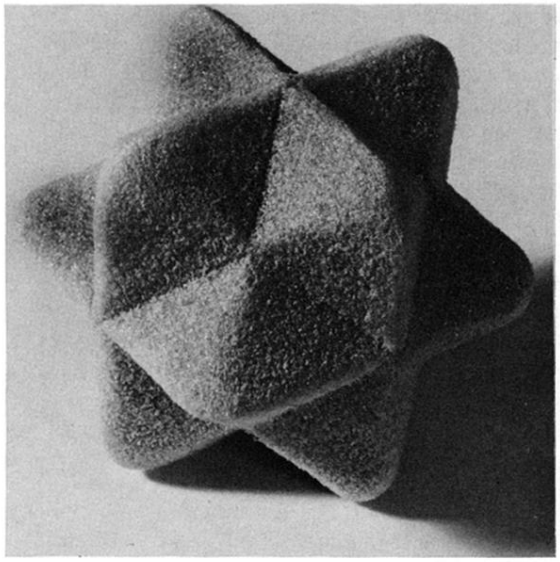

FIG. 4. Model of the Γ5 sheet in Ir.